Features of air masses associated with the deposition of Pseudomonas syringae and Botrytis cinerea by rain and snowfall.

Caroline Monteil, Marc Bardin, Cindy E. Morris

Short title: *P. syringae* and *B. cinerea* in precipitation

Features of air masses associated with the deposition of *Pseudomonas syringae* and *Botrytis cinerea* by rain and snowfall.

Caroline L. MONTEIL, Marc BARDIN and Cindy E. MORRIS*

INRA, UR0407 Pathologie Végétale, F-84143 Montfavet cedex, France
*Corresponding author. Tel.: +33 (0)4 32 72 28 86; fax: +33 (0)4 32 72 28 42; E-mail: Cindy.Morris@avignon.inra.fr

Subject category: Microbial population and community ecology

Key words: ice nucleation activity, HYSPLIT, landscape ecology, long distance dissemination, aerobiology

ABSTRACT

Clarifying the role of precipitation in microbial dissemination is essential for elucidating the processes involved in disease emergence and spread. The ecology of *Pseudomonas syringae* and its presence throughout the water cycle makes it an excellent model to address this issue. In this study, 90 samples of freshly fallen rain and snow collected from 2005–2011 in France were analyzed for microbiological composition. The conditions favorable for dissemination of *P. syringae* by this precipitation were investigated by (i) estimating the physical properties and backward trajectories of the air masses associated with each precipitation event and by (ii) characterizing precipitation chemistry, and genetic and phenotypic structures of populations. A parallel study with the fungus *Botrytis cinerea* was also performed for comparison. Results showed that (i) the relationship of *P. syringae* to precipitation as a dissemination vector is not the same for snowfall and rainfall, while it is the same for *B. cinerea* and (ii) the occurrence of *P. syringae* in precipitation can be linked to electrical conductivity and pH of water, the trajectory of the air mass associated with the precipitation and certain physical conditions of the air mass (i.e. temperature, solar radiation exposure, distance travelled), whereas these predictions are different for *B. cinerea*. These results are pertinent to understanding microbial survival, emission sources and atmospheric processes and how they influence microbial dissemination.

INTRODUCTION

To optimize the scenarios that predict the risks associated with the emergence and spread of disease, epidemiologists need to understand the complete process of pathogen dissemination and survival. But more fundamentally, describing the dissemination pathways of plant pathogens and microorganisms reveals the range of environmental contexts that structure populations. For aerial plant pathogens, knowledge about the favorable or limiting conditions controlling their dissemination through the atmosphere from local to global scales determines the success of predictions and thereby of the management of the plant diseases they cause.

Mechanisms of aerial dissemination have been well documented for fungi and bacteria from several meters near the Earth's surface up to several kilometers into the troposphere (see reviews by Gregory (1961) and Burrows *et al.* (2009)). Atmospheric dissemination involves three processes: (i) emission from a source, (ii) transport and survival in the atmosphere via the circulation of air masses and (iii) deposition back to Earth's surface through impaction, turbulent airflows or precipitation. For obligate biotrophs such as rusts that grow on a limited number of well-known host plants, the inoculum source and time of emission often can be identified, leading to rather clear descriptions of their atmospheric movements across continents and oceans and to the elucidation of a link between source and sink populations (Isard *et al.*, 2005, Krupa *et al.*, 2006, Nagarajan and Singh 1990, Pan *et al.*, 2006, Purdy *et al.*, 1985, Tao *et al.*, 2009, Wang *et al.*, 2010). But for non-obligate pathogens with wide host ranges and saprophytic phases of growth, it is difficult to link the populations deposited by precipitation or dry sediments to a specific source, thereby complicating inference of their dissemination trajectory (Morris *et al.*, 2014b).

Consequently, constructing dissemination trajectories for such organisms involves compiling corroborative evidence from the time frame and geographic contexts of possible backward trajectories that are calculated from the end point of deposition (Prospero *et al.*, 2005). Tools are available for modeling the trajectories of air masses and they have been applied to evaluating the long distance dissemination of various fungal pathogens and insect vectors of plant disease (Aylor *et al.*, 2011, Davis 1987, Pan *et al.*, 2006, Pfender *et al.*, 2006, Prospero *et al.*, 2005, Zhu *et al.*, 2006). For microorganisms with a multitude of possible emission sources, such tools have been recently applied to describe the global dispersion of airborne bacteria and archaea with winds (Smith *et al.*, 2013). *Pseudomonas syringae* and *Botrytis cinerea* are prime examples of such microorganisms for which dissemination history cannot be observed directly. These plant pathogens generate losses on a wide range of crops, e.g., on kiwifruit, horse chestnut, or tomato for *P. syringae* (Kunkeaw *et al.*, 2010, Mazzaglia *et al.*, 2012, Webber *et al.*, 2008), or on tomato, raspberry and wine grapes for *B. cinerea* (Williamson *et al.*, 2007). Both of these plant pathogens are aerially disseminated, have a saprophytic lifestyle and include many lineages characterized by wide host range (Holz *et al.*, 2004, Morris *et al.*, 2008). Both have been isolated from clouds as well (Amato *et al.*, 2007). But they have fundamentally different traits that could have an impact on their deposition. Firstly, *P. syringae* has the ability to nucleate ice formation (Lindow 1983, Möhler *et al.*, 2008, Wolber *et al.*, 1986), thereby inciting conditions propitious for the formation of precipitation leading to deposition of the bacterium from the troposphere (Morris *et al.*, 2008, Morris *et al.*, 2010). To date, *B. cinerea* has been reported to not be ice nucleation (IN) active (Delort *et al.*, 2007) and therefore cannot incite its own deposition in the same way. Secondly, bacterial cells are at least ten-fold smaller than most fungal spores: *P. syringae* is about 1 µm in length (Monier and Lindow 2003) whereas conidia of *B. cinerea* are > 10µm in diameter (Pezet and Pont 1990). These two properties, particle size and nucleation properties, are determining factors in

the processes that lead to removal of microorganisms from the atmosphere with precipitation (Flossmann *et al.*, 1985, Pruppacher and Klett 1997, Rodhe and Grandell 1972, Rogers and Yau 1989). Small particles such as the cells of *P. syringae* cells are likely to be uplifted into clouds and eventually incorporated into cloud droplets. Their precipitation can be assured if crystallization of droplets occurs —a process that can be enhanced via the IN activity of these bacteria. Larger particles such as spores of *B. cinerea* will have shorter upward trajectories on average and many of the spores are likely to be washed out from the atmosphere by impaction with drops below the cloud. For these and all other non-obligate biotrophic plant pathogens, the role of precipitation as a dissemination vector, the capacity of these organisms to survive during the trajectory and the dissemination history of air masses leading to precipitation have never been explored.

In this study, we characterized the deposition of *P. syringae* and *B. cinerea* in snowfall and rainfall sampled between 2005 and 2010 in Southern France. For 90 such samples, the abundance, IN activity and population structure of *P. syringae* were determined and pH and electrical conductivity were measured. Then, we inferred the dissemination trajectories of *P. syringae* by comparing these observations to backward trajectories and the associated climatic parameters computed under the HYSPLIT–4 model (Draxler and Hess 1998). Finally, the conditions associated with the occurrence of *P. syringae* in precipitation were compared to those linked to the presence of the fungus *B. cinerea* (evaluated in a subset of the samples) to identify the conditions of deposition specific to each plant pathogen. This multidisciplinary approach, associating meteorological computations and microbial ecology, provides clues about the processes and conditions of their dissemination trajectories.

MATERIALS AND METHODS

Sampling of snowfall and rainfall.

The field study was conducted from Dec. 2005 to Nov. 2011 at 14 sites mostly in southern France (Table 1). Samples were collected from a total of 25 fresh rainfalls and 65 fresh snowfalls by procedures that avoided contamination from local sources. Events are defined to be independent if they occurred at separate sampling sites or if there was at least a 24 h time lapse between the end of a precipitation event and the beginning of the next one. Details about samples are given in Table S1. They were collected either in sterile plastic tubs (for rain) or on clean plastic tarps (1 m^2) (for snow) that had been placed and elevated from the ground in situations where the snowfall event was anticipated. Rain collector tubs were 1m tall and elevated to protect the rain samples from contamination by rain-splashed soil. Samples were recovered from the samplers no later than 3h after the end of the snowfall event or when at least 200 – 500 ml of rainwater accumulated. Samples were transported in a cooler to the laboratory, kept at 4°C and processed within 24 hours. Electrical conductivity (EC) and pH were measured directly in an aliquot of the unprocessed sample with an electrochemical analyzer (Consort C561, UK, reference temperature at 25°C). EC and pH values had an accuracy of ± 1µS cm^{-1} and ± 0.01 pH unit, respectively.

Quantification of microorganisms

Snow samples were thawed overnight at 21°C. Snowmelt and rainwater were processed within 24 h as described previously (Morris *et al.*, 2008). Samples were concentrated 200 times by filtration across sterile nitrous cellulose filters (pore diameter 0.22 µm) before dilution plating. *P.*

syringae and total culturable bacteria were enumerated in all samples and *B. cinerea* in 29 samples as described below (Table 1).

The concentrated samples were dilution-plated on King's medium B supplemented with boric acid, cephalexin and cycloheximide (KBC) to enumerate *P. syringae* (Mohan and Schaad 1987) and on 10% tryptic soy agar (TSA) for total mesophilic bacteria. Plates were incubated for up to 5 days at 22–25°C. Up to 30 strains of *P. syringae* chosen randomly from a single dilution were purified from each sample. Putative strains of *P. syringae* were tested for production of fluorescent pigment on King's medium B (King *et al.*, 1954), for the absence of arginine dihydrolase and of cytochrome C oxidase as described previously (Morris *et al.*, 2008). A set of 513 strains of *P. syringae* were stored at –80°C in nutrient broth with 40% glycerol for further characterization.

For *B. cinerea*, aliquots were plated on selective Botrytis Spore Trap medium (BSTM) (Edwards and Seddon 2001). The number of developing colonies of *B. cinerea* was recorded daily during 14 days of incubation at 20°C and colonies were transferred to PDA medium as described by Leyronas and Nicot (2013). Strains were maintained in stock cultures at –20°C in a glycerol-phosphate buffer 0.06 M (50/50, vol/vol for further characterization. The detection thresholds were 5 colony-forming units (CFU) L^{-1} for the targeted plant pathogens, and 55 CFU L^{-1} for total bacteria. This difference in threshold was due to the fact that 10 times more replicates of each dilution were plated on KBC and BSTM than on TSA to assure detection of the pathogens. A set of 83 *B. cinerea* strains was stored for further characterization.

Characterization of trajectories and climatic conditions of air masses

The trajectories and the associated climatic conditions of air masses arriving at the sampling location on the day of the precipitation event were determined with the HYSPLIT model version 4 (HYbrid Single-Particle Lagrangian Integrated Trajectory, http://ready.arl.noaa.gov/ready/HYSPLIT4.html). This model, developed by NOAA Air Resources Laboratory and Australia's Bureau of Meteorology, uses previously gridded meteorological data to calculate forward and backward trajectories and the associated climatic conditions and provides simulations for atmospheric particle dispersion and deposition (Draxler and Hess 1998, Draxler and Rolph 2011). The backward trajectories of air masses for each precipitation event were determined for the periods of 24 h, 48 h and 120 h preceding the event for endpoint elevations of 50, 500 and 1000 m above ground level (AGL). These altitudes represent a vertical section of the planetary boundary layer defined by Gregory (1961). Hourly climatic parameters were also obtained from the database including precipitation (mm), sun flux (W m^{-2}), relative humidity (%), pressure (hPa), altitude (m) and temperature (°C). The meteorological data GDAS (Global Data Assimilation System) used by this model were produced by the National Center for Environmental Prediction. The total distance traveled by air masses (km) was determined under POSTGRESQL/POSTGIS (http://www.postgresql.org) and the map projections were made with Quantum GIS version 1.7. 0 (Quantum GIS Development Team 2011).

Statistical analyses

Statistical analyzes were performed with data from all samples (n=90) for *P. syringae* and from 29 samples for comparisons of the two pathogens using the R software version 2.9.1 (The R Development Core Team 2011). To compare abundances of the pathogens between samples when they were detected, values for population density were $\log_{10}$ transformed prior to calculations.

Phenotypic and genotypic characterization of microorganisms

All *P. syringae* and *B. cinerea* strains were characterized for their IN activity in distilled water as described previously (Morris *et al.,* 2008). IN activity was evaluated by determining the freezing temperature, between –2° and –8°C of three 30 µL drops each containing 10^6 cells or spores and was scored positive if at least two drops froze. The pathogenicity of bacterial strains was determined by testing for the presence of the Type III Secretion System, a key factor in virulence (Cunnac *et al.,* 2009). This involved testing for the capacity to induce a hypersensitive reaction (HR) in tobacco leaves (*Nicotiana tabacum* cv. Xanthi) as described previously (Morris *et al.,* 2008). Utilisation of D(–)tartrate was also characterized because this trait is rare among *P. syringae* (Sands *et al.,* 1970) and therefore could provide a means to discriminate among certain biotypes. The pathogenicity of the fungus was determined by testing its ability to induce symptoms on tomato, one of its known hosts. The aggressiveness of *B. cinerea* strains on tomato plants (cv. Monalbo) was determined as described in Ajouz *et al.* (2010) by inoculating stems with a calibrated spore suspension (10^6 spores mL^{-1}). Lesion length was monitored on 3 plants for 7 days and the whole experiment was repeated three times. The Area Under the Disease Progress Curve (AUDPC) was computed as described by Decognet *et al.* (2009). To facilitate the comparison of aggressiveness between strains, a relative aggressiveness index (in percent) was computed as the ratio between the average AUDPC of the tested strain and that of the reference strain BC1.

Morris *et al.* (2010) showed that phylogeny reconstruction based on the gene for citrate synthase (*cts*) allows identification of groups within the *P. syringae* species complex. For 209 randomly chosen strains (about 11 per sample), the *cts* gene was sequenced and then strains were classified as described previously (Monteil *et al.,* 2012, Morris *et al.,* 2010) to characterize the genetic structure of the *P. syringae* population.

Inference of population structures by landscape clustering

We determined the spatial population structure of *P. syringae* to test the hypothesis that genetic diversity of *P. syringae* populations in precipitation is different according to the sampling zone. We used a clustering model: GENELAND version 4.0.2 under R software (Guillot *et al.,* 2005a, 2005b, 2012) to (i) estimate the number of panmictic clusters (*k*), (ii) assign to each genetic cluster a membership to a sampling zone and (iii) assign individual strains to a cluster. The clustering approach can combine data on genotypic polymorphism with geographic coordinates projected on a rasterized map. The optimal number of clusters *k* and the posterior probabilities of cluster membership for any unit of the sampling map were identified by a Markov chain Monte Carlo procedure (MCMC) under the assumption that there is no admixture between populations and that populations are at Hardy-Weinberg equilibrium with linkage equilibrium between loci (HWLE) (Guillot *et al.,* 2012). Here, we assumed that allele frequencies of the *cts* gene were independent between samples. We thus used the Uncorrelated model (UFM), applied the default settings and performed 500 000 iterations with an initial $k = 10$ and a burning-in period of 50 000 iterations. A second iteration of the calculation was then performed with a fixed number K. Strains were assigned to a cluster according a threshold of membership coefficient of $q > 0.9$.

RESULTS

The occurrence of *P. syringae* in precipitation is correlated with chemical properties of precipitation and the associated air mass trajectories

P. syringae was detected in 25 of the 90 precipitation samples analyzed (snow and rain combined) with population sizes varying between 10^2 and 10^6 CFU L^{-1} when detected (Figure 1 and Supplementary Table S1). Each air mass trajectory was classified according to the three geographical sectors defined by Celle-Jeanton *et al.* (2009) for precipitations in southeastern France: West (region 1), North and East (region 2) and Mediterranean (region 3) (Figure 2a). Among our samples, air masses came more frequently from region 2 compared to those from the other regions (Figure 2b). However, they carried *P. syringae* significantly less frequently (12 %) than air masses from the other regions (37 % and 46 %) (pairwise Fisher's exact test, $P < 0.05$). Concerning the chemistry of the precipitations, those carrying *P. syringae* had significantly higher conductivities (13 ± 2 vs. 8 ± 1 µS cm^{-1}) and were more alkaline (pH 6.22 ± 0.08 vs. 5.76 ± 0.23) than those in which *P. syringae* was not detected (Mann-Whitney U, $P < 0.05$). Overall, precipitation from region 3, which carries *P. syringae* more often than precipitation from other regions, had significantly higher conductivity than precipitation from the other two regions (Multiple MWU, $P < 0.05$).

Aggregate means of climatic parameters of air masses preceding the precipitation events were compared for samples carrying and not carrying *P. syringae* for the three periods and elevations mentioned above. An example of typical results obtained is shown in Figure 3 for the 48 h period. All data are provided in Table 2. On the whole, results for comparisons for the three periods and three elevations were consistent, with a better discrimination for the shorter periods and lower elevations. The cumulative solar radiation, temperature, pressure and distance travelled by the air masses were significantly greater when *P. syringae* was detected in precipitation than when it was absent (MWU, $P < 0.05$). Mean altitude and relative humidity of the air masses during their trajectories did not have a consistently significant effect on the presence of *P. syringae* in precipitation, but when their effects were significant, the values for these parameters were smaller when the bacterium was detected compared to when it was absent. Sun flux, temperature, altitude and pressure were inter-correlated (Spearman, $P < 0.001$) as expected. No significant effects of cumulative rainfall during the trajectory on the occurrence of *P. syringae* were observed.

Air mass trajectory and climatic properties associated with the occurrence of *B. cinerea* in precipitation are different from those associated with *P. syringae*

For the subset of samples analyzed for both pathogens, *B. cinerea* was detected in precipitation at twice the rate of *P. syringae* (62.1 % vs. 34.5 %, Fisher-exact test, $P = 0.06$) (Table 3). In contrast with *P. syringae*, *B. cinerea* was present in precipitation that was more acidic than samples in which the fungus was not detected (5.80 ± 0.11 vs. 6.31 ± 0.17, MWU test, $P = 0.13$) and its presence was not linked to temperature and pressure (MWU test, $P > 0.25$). However, for the 50 m elevation at 24 h and 48 h prior to the sampled precipitation event, the presence of *B. cinerea* was linked to higher rainfall rates and higher maximum relative humidity experienced along the air mass trajectory before the sample was collected (Supplementary Table S2). No significant difference was observed among the different origins of air masses in terms of the frequency of precipitations carrying *B. cinerea* (43, 67 and 75% of air masses from regions 1, 2 and 3, respectively). However, the frequency of the pathogens in precipitation from region 2 was five times higher for *B. cinerea* than for *P. syringae* (Fisher-exact test, $P < 0.05$).

Populations of *P. syringae*, but not of *B. cinerea*, are disseminated differently by snow and rain and display distinct phenotypic patterns in these substrates

P. syringae was carried more frequently, but at lower concentrations, by rain than by snowfall. There was a significant effect of the type of precipitation on the occurrence of *P. syringae*, with 68 % of the rain events carrying the bacterium vs. 12% of snowfalls (Table 3). However the population densities of the bacterium in snowfall were on average ten-fold greater than in rain. For total bacteria the opposite trend was observed with snowfall carrying 10% of the population densities observed in rainfall (Table 4). For the subset of samples used to compare the two pathogens, this result was slightly less marked for *P. syringae*, and for *B. cinerea* no differences in frequency and population size were observed between rain and snowfall (Tables 3 and 4). Overall, the abundances of *B. cinerea* spores in precipitation were 100-fold smaller than those of *P. syringae* CFU (MWU, $P < 0.001$).

All *B. cinerea* strains were able to infect tomato petiole stubs and to generate symptoms on the stem of tomato plants. The aggressiveness index for the 83 strains tested ranged from 11% to 144% (compared to the reference strain BC1). No differences between strains from rain and snow were detected. Finally, none of the strains of *B. cinerea* tested were IN active at temperatures warmer than –9°C (Table 4).

In contrast, the phenotypic structure of *P. syringae* populations was highly influenced by the type of precipitation. All strains of *P. syringae* in snow were IN active and induced HR in tobacco whereas rain contained some strains incapable of IN activity or inducing HR. However, for the IN active strains from these two types of precipitation, there was no significant difference in their freezing onset temperature. Strains from rain more frequently were capable of metabolizing D(−)tartrate compared to those from snow (Table 4). In addition to its strong relationship with the frequency of strains inducing HR on tobacco, frequency of IN active strains was also significantly correlated with minimum pressure experienced by the air mass and the distance it travelled (Table 5), but not with other climatic parameters (data not shown).

Population structure of *P. syringae* is associated with the location and type of precipitation

There were sufficient numbers of strains of *P. syringae* from rain and snowfall to assess the effect of precipitation type on genetic population structure. However, this is was not the case for *B. cinerea*. Therefore analysis of the influence of the type of precipitation on genetic population structure was conducted only for *P. syringae*.

The *cts* sequences (427 base pairs, 80 SNPs) of the 209 strains of *P. syringae* selected randomly from snow and rain represented 54 unique haplotypes. Half of the haplotypes were represented by only one strain in the whole sample, and the three dominant haplotypes were represented by 28, 22 and 19 strains. GENELAND estimated that there were three clusters (k) whether spatial coordinates were included or not. These latter results were consistent with those obtained using the STRUCTURE 2.3 software (Falush *et al.*, 2003, Pritchard *et al.*, 2000) (data not shown). Assuming admixture between populations, 89% of the haplotypes clearly belonged to only one cluster ($q > 0.95$), indicating that the three clusters were highly divergent. As shown in Figures 4a to 4d, each cluster corresponded to a distinct spatial domain covering several sampling sites that are geographically close. Half of the strains belonged to cluster 3 that was specific to rain (Figure 4e). Cluster 1 was represented by strains of group 2 defined by Sarkar and Guttman (2004) for which at least one strain was present in each sample, with a higher proportion in snow (Figure 5).

DISCUSSION

Our work provides new insight into the role of precipitation in the dissemination of air-borne plant pathogens and the unique opportunity to estimate the fluxes of plant pathogens due to precipitation over crops. Based on the hydrological fluxes of snowfall and rainfall estimated by Oki and Kanae (2006), and our estimates of the frequency of precipitation carrying *P. syringae* and the mean concentration, we can estimate that up to 10^{20} cells of this bacterium could be deposited by rain and 10^{19} cells by snowfall across the world every year. Considering a hypothetical but realistic situation where (i) a single rain event of 20 mm would bring 10^7 cells of *P. syringae* / ha of field, (ii) a leaf area index of a given crop of 1, and (iii) that every cell fell on a leaf, such precipitation would bring only 1 CFU / 100 cm² of leaf (i.e. 1 cell for about 5-10 leaves). Compared to the populations brought by irrigation water, this is much less important. Irrigation retention basins can contain 100 CFU L^{-1} of *P. syringae* pv. *aptata* (Riffaud and Morris 2002). Therefore, a single irrigation event (2×10^5 L ha^{-1}) would transfer a total of $1.36 \times 10^6 – 4.06 \times 10^6$ CFU per ha of crop for an equivalent of 5 to 15 cells per leaf. The same calculation for *B. cinerea* leads to estimates of fluxes of the same order of magnitude.

The role of precipitation in the long distance dissemination of plant pathogens is still poorly understood. Here, we showed that the presence of *P. syringae* in precipitation is statistically linked to biological, chemical and climatic parameters of the precipitation water and the air mass that carried it. In particular, the probability of *P. syringae* deposition with precipitation can be inferred by determining air mass characteristics (i.e. temperature, sun flux, origin, distance travelled) and precipitation pH/conductivity. It is unlikely that such trends would be apparent and particularly the trends linked to air mass origin if the deposition of *P. syringae* with precipitation were due primarily to the incorporation of local and near surface air-borne cells by impaction with precipitation droplets (scrubbing). The comparison with *B. cinerea*, whose presence in precipitation is indifferent to air mass origin, is important evidence that a major part of the cells of *P. syringae* in precipitation originates from the air mass at cloud height whereas the presence of *B. cinerea* is more likely due to below-cloud scrubbing. Overall, differences in frequency of occurrence of the two pathogens in precipitation support that they have different sensitivities to the climatic conditions regulating their incorporation into precipitation: (i) *P. syringae* is favored by warm conditions while *B. cinerea* is favored by high humidity and colder temperatures and (ii), presence of *P. syringae* in precipitation is promoted by alkaline precipitation while that of *B. cinerea* is promoted by acidic precipitation. Furthermore, snowfall and rainfall are not equal in their capacity to deposit *P. syringae*, but they are both equally efficient in depositing *B. cinerea*.

The relationships between pathogen deposition and environmental conditions raise questions about their causes. Do they indicate differences in (i) atmospheric survival rate relative to chemical and physical conditions, (ii) the strength of emission sources and/or (iii) the atmospheric processes regulating their transport? Distinguishing the effects of all sources of variation is challenging because the occurrence of a microorganism in precipitation is likely multifactorial. Scrubbing of the atmosphere below cloud level is one factor that could contribute to the presence of microorganisms in precipitation. Washout and impaction by falling precipitation below the cloud is the most efficient scavenging process for non-IN active particles larger than 10 µm such as spores of *B. cinerea* whereas it is negligible for particles smaller than 4 µm (Burrows *et al.*, 2009, Gregory 1961, Mircea *et al.*, 2000, Pezet and Pont 1990, Rodhe and Grandell 1972). Therefore, below-cloud scavenging of *P. syringae* by precipitation is likely to be low – except for cells on debris or on spores – whereas it could be important for *B. cinerea*.

Based on the reasoning above, it is likely that a large part of the cells of *P. syringae* in precipitation collected at ground level are in the precipitating air masses at cloud height. The presence of *P. syringae* in clouds is well established (Amato *et al.*, 2007, Joly *et al.*, 2013, Sands *et al.*, 1982). Therefore, it is legitimate to consider how our results make sense in terms of atmospheric and cloud physics. For example, the positive correlations between the occurrence of *P. syringae* in precipitation and temperature, sun flux and air pressure might simply suggest that low temperatures could be detrimental to the survival of *P. syringae* in the atmosphere. However, these observations are likely to be associated with the natural seasonal solar and temperature cycles that regulate bacterial emission into the planetary boundary layer (Lighthart 1999). Solar radiation heats surfaces and creates thermal convective updrafts lifting epiphytic and soil bacteria into the atmosphere following solstices and diurnal patterns (Lighthart 1997, 1999, Lindemann *et al.*, 1982, Tong and Lighthart 2000). This process is more efficient for formation of bacterial than for fungal aerosols. Fungi may release spores in the atmosphere independently of solar radiation – e.g., by puff or tap mechanisms. Interestingly, we found several parameters of humidity to be related to the presence of *B. cinerea* in precipitation that are also associated with its emission into the atmosphere (Leyronas and Nicot 2013). On the other hand, our results (Table 5) support the hypothesis that warmer temperature may select ice nucleation active *P. syringae* in the atmosphere and promote its deposition. Indeed precipitation would be more efficiently catalyzed by the pathogen at warm temperatures when non-biological ice nucleators are not efficient (Morris *et al.*, 2014a).

The multiple possible sources of non-obligate biotrophs such as *P. syringae* and *B. cinerea* and their long-range transport ability through the atmosphere make it almost impossible to track dissemination history. Each cell or spore in a precipitation event might have different dissemination histories both in terms of trajectory and exposure to selection pressures. Here, we addressed that question through the sampling of precipitation at different locations in natural habitats upstream of crop areas and downstream within a catchment basin. Sampling effort was highly dependent on weather forecasts and on access to locations where precipitation occurred thereby adding a possible bias. Future studies should target the role of landscape structure and attempt to distinguish it from that of the underlying atmospheric processes on microbial deposition with precipitation. Tackling the tracing of dissemination history will require appropriate sampling strategies: this will require the sampling of not only precipitations, but of the suspected local emission sources as well — e.g., canopies, grasslands, crops and watersheds. Equally important, such a challenge requires identifying the right molecular indicators. Appropriate indicators will be source specific and they must persist in microbial cells at the same time scale as the duration of the transport process.

Precipitation chemistry might give insight into processes involved in transport with rain and snowfall. *P. syringae* is favored by moderately alkaline conditions while *B. cinerea* prefers acid conditions (Manteau *et al.*, 2003). Recently, Attard *et al.* (2012) showed that acidic pH had a negative impact on the IN activity of *P. syringae* and thus possibly on its deposition. Thus, we can assume that acid pH in clouds decreases *P. syringae* deposition. However alkaline pH and relatively higher electrical conductivities are indicators of minerals in the atmosphere and notably of dusts (aluminum and calcite) (Delmas *et al.*, 1996, Lee *et al.*, 2000, Ozsoy and Saydam 2000). The presence of dusts associated with microorganisms has been reported in clouds, air and precipitation, where dust plays a protective role against the extreme conditions in the atmosphere (e.g. UV, desiccation) (Griffin *et al.*, 2002, Hara and Zhang 2012, Harrison *et al.*, 2005, Kellogg and Griffin 2006, Maki *et al.*, 2008, Prospero *et al.*, 2005). Therefore, our observations could be the result of the presence of dust acting as a shelter for *P. syringae* during atmospheric transport.

Interestingly, air masses with the most alkaline and conductive precipitation originate from the Iberian Peninsula where Southerly winds are known to transport a large amount of solid particles, essentially calcite dusts coming from the Sahara (Delmas *et al.*, 1996, Kellogg and Griffin 2006, Loye-Pilot and Morelli 1988). Winds can increase upward fluxes of soil dusts in the atmosphere. Among the parameters we used to characterize air mass movement, the total distance traveled in a given time period by an air mass is an indication of its average speed. Although distance traveled did not have a significant effect on the presence of the two targeted pathogens, distance traveled was consistently greater when they were present.

Population genetic structure might also be useful in elucidating trajectory. Here, the clustering of microbial diversity in precipitation over space suggested that *P. syringae* populations in precipitation would be influenced more by local sources than by distal sources. Indeed, if local sources were not dominant, we could expect more numerous sources and consequently a more complex and mixed population structure. But we cannot exclude that the structure of *P. syringae* populations along the landscape is the result of a bottleneck exerted by atmospheric processes. A set of genotypes and IN activity is closely linked with each type of precipitation. Thus selection of IN active populations could be at the origin of the differences between the genotypic patterns we observed. Our experimental data for *P. syringae* and *B. cinerea* and their biology are congruent with the predictions made by atmospheric physics concerning the removal of particles by precipitation in relation to particle size and nucleation/condensation properties and cloud physics (Flossmann *et al.*, 1985, Pruppacher and Klett 1997, Rodhe and Grandell 1972, Rogers and Yau 1989). At mid-latitudes, snow is initiated by an ice crystal-process; snowflakes arise from crystals that are initiated by ice nuclei and then aggregate (Rogers and Yau 1989). A particle smaller than 1µm such as *P. syringae* (Monier and Lindow 2003) can be incorporated in a snowflake if it is IN active (Rodhe and Grandell 1972). For rainfall at mid-latitudes however, two different processes can lead to rain droplet formation. Rain can begin as ice via the same process described above if temperatures in clouds are sufficiently cold. However, under warmer conditions and when there is sufficient turbulence, rainfall can be initiated by a coalescence process that involves condensation nuclei, growth of ice particle by collision with supercooled droplets and melting in the lower zone of the cloud (Rogers and Yau 1989). In this case, particles can be incorporated into rainfall within the cloud independent of their IN activity (Rodhe and Grandell 1972). These phenomena are coherent with our observation that 100% of *P. syringae* strains in snow are IN active whereas this is not the case for those in rainfall and might also contribute to enhancing the abundance of IN active bacteria in snow compared to that in rain. *B. cinerea* is not IN active and therefore would not benefit from the role of ice crystal formation in rain or snow. Interestingly, there is no difference between rain and snow in the concentrations of *B. cinerea*. However other phenomena related to the physics of rainfall might be important for this fungus.

It is important to understand how pathogens, and microbes in general, disseminate and to identify the processes structuring their populations. Overall, our estimation of atmospheric fluxes and our results about diversity give new insights into the role of precipitation in the dynamics of air-borne microbial populations. They suggest that precipitation contributes to metapopulation mixing over short and long-range distances, and to triggering microbial growth through rain splashing (Fitt *et al.*, 1989, Hirano *et al.*, 1996), rather than contributing directly to the size of microbial populations on crops. For IN active microorganisms, this dissemination can be part of a feedback process between land cover and the atmosphere (Morris *et al.*, 2014a). The link between landscape structure, precipitation and atmosphere, and the time scale interactions that occur, remain to be

investigated to better understand microbial population dynamics over time and space and to identify the selection pressures that contribute to their evolution.

ACKNOWLEDGMENTS

We thank Daniel Granier and his team from the Super Sauze ski resort, for help with collection of samples. We are grateful to Odile Berge (INRA, Avignon) for her help in sampling and for enriching discussions, to Ghislain Géniaux and Michel Mourly (INRA, Avignon) for help with spatial analysis of the trajectories, and to Vaughan Phillips for his insights in cloud physics. The authors gratefully acknowledge Claire Troulet for excellent technical assistance for the *Botrytis cinerea* experiments.

Supplementary information is available at The ISME Journal's website (http://www.nature.com/ismej)

The authors of this work declare no conflict of interest.

REFERENCES

Ajouz S, Nicot PC, Bardin M (2010). Adaptation to pyrrolnitrin in *Botrytis cinerea* and cost of resistance. *Plant Pathol* **59:** 556-566.

Amato P, Parazols M, Sancelme M, Laj P, Mailhot G, Delort AM (2007). Microorganisms isolated from the water phase of tropospheric clouds at the Puy de Dome: major groups and growth abilities at low temperatures. *FEMS Microbiol Ecol* **59:** 242-254.

Attard E, Yang H, Delort AM, Amato P, Poeschl U, Glaux C *et al* (2012). Effects of atmospheric conditions on ice nucleation activity of *Pseudomonas*. *Atmos Chem Phys* **12:** 10667–10677.

Aylor DE, Schmale DG, Shields EJ, Newcomb M, Nappo CJ (2011). Tracking the potato late blight pathogen in the atmosphere using unmanned aerial vehicles and Lagrangian modeling. *Agr Forest Meteorol* **151:** 251-260.

Burrows SM, Elbert W, Lawrence MG, Poschl U (2009). Bacteria in the global atmosphere - Part 1: Review and synthesis of literature data for different ecosystems. *Atmos Chem Phys* **9:** 9263-9280.

Celle-Jeanton H, Travi Y, Loye-Pilot MD, Huneau F, Bertrand G (2009). Rainwater chemistry at a Mediterranean inland station (Avignon, France): Local contribution versus long-range supply. *Atmos Res* **91:** 118-126.

Cunnac S, Lindeberg M, Collmer A (2009). *Pseudomonas syringae* type III secretion system effectors: repertoires in search of functions. *Curr Opin Microbiol* **12:** 53-60.

Davis JM (1987). Modeling the long-range transport of plant pathogens in the atmosphere. *Annu Rev Phytopathol* **25:** 169-188.

Decognet V, Bardin M, Trottin-Caudal Y, Nicot PC (2009). Rapid change in the genetic diversity of *Botrytis cinerea* populations after the introduction of strains in a tomato glasshouse. *Phytopathology* **99:** 185-193.

Delmas V, Jones HG, Tranter M, Delmas R (1996). The weathering of aeolian dusts in alpine snows. *Atmos Environ* **30:** 1317-1325.

Delort A-M, Amato P, Sancelme M, Morris CE, Laj P (2007). Isolation of ice-nucleation active microorganisms from cloud water. *Proceedings of the XXIV International Union of Geodesy and Geophysics (IUGG) General Assembly. Earth: our changing planet.*; July 2-13, 2007; Perugia (Italy).

Draxler RR, Hess GD (1998). An overview of the HYSPLIT_4 modelling system for trajectories, dispersion and deposition. *Aus Meteorol Mag* **47:** 295-308.

Draxler RR, Rolph GD (2011). HYSPLIT (HYbrid Single-Particle Lagrangian Integrated Trajectory) Model access via NOAA ARL READY website (http://ready.arl.noaa.gov/HYSPLIT.php). *NOAA Air Resources Laboratory, Silver Spring, MD*.

Edwards SG, Seddon B (2001). Selective media for the specific isolation and enumeration of *Botrytis cinerea* conidia. *Lett Appl Microbiol* **32:** 63-66.

Falush D, Stephens M, Pritchard JK (2003). Inference of population structure using multilocus genotype data: Linked loci and correlated allele frequencies. *Genetics* **164:** 1567-1587.

Fitt BDL, McCartney HA, Walklate PJ (1989). The role of rain in dispersal of pathogen inoculum. *Annu Rev Phytopathol* **27:** 241-270.

Flossmann AI, Hall WD, Pruppacher HR (1985). A theoritical study of the wet removal of atmospheric pollutants. Part 1: The redistribution of aerosol particles captured through nucleation and impaction scavenging by growing cloud drops. *J Atmos Sci* **42:** 583-606.

Gregory PH (1961). *The microbiology of the atmosphere*. Interscience Publishers, Inc., New York.

Griffin DW, Kellogg CA, Garrison VH, Shinn EA (2002). The global transport of dust - An intercontinental river of dust, microorganisms and toxic chemicals flows through the Earth's atmosphere. *Am Sci* **90:** 228-235.

Guillot G, Estoup A, Mortier F, Cosson JF (2005a). A spatial statistical model for landscape genetics. *Genetics* **170:** 1261-1280.

Guillot G, Mortier F, Estoup A (2005b). GENELAND: a computer package for landscape genetics. *Mol Ecol Notes* **5:** 712-715.

Guillot G, Renaud S, Ledevin R, Michaux J, Claude J (2012). A unifying model for the analysis of phenotypic, genetic and geographic data. *Syst Biol* **61:** 897-911.

Hara K, Zhang D (2012). Bacterial abundance and viability in long-range transported dust. *Atmos Environ* **47:** 20-25.

Harrison RM, Jones AM, Biggins PDE, Pomeroy N, Cox CS, Kidd SP *et al* (2005). Climate factors influencing bacterial count in background air samples. *International Journal of Biometeorology* **49:** 167-178.

Hirano SS, Baker LS, Upper CD (1996). Raindrop momentum triggers growth of leaf-associated populations of *Pseudomonas syringae* on field-grown snap bean plants. *Appl Env Microbiol* **62:** 2560-2566.

Holz G, Coertze S, Williamson B (2004). The ecology of Botrytis on plant surfaces. In: Elad Y, Williamson B, Tudzynski P, Delen N (eds). *Botrytis: Biology, pathology and control*: Dordrecht, The Netherlands: Kluwer. pp 9–24.

Isard SA, Gage SH, Comtois P, Russo JM (2005). Principles of the atmospheric pathway for invasive species applied to soybean rust. *Bioscience* **55:** 851-861.

Joly M, Attard E, Sancelme M, Deguillaume L, Guilbaud C, Morris CE *et al* (2013). Ice nucleation activity of bacteria isolated from cloud water. *Atmos Environ* **70:** 392-400.

Kellogg CA, Griffin DW (2006). Aerobiology and the global transport of desert dust. *Trends Ecol Evol* **21:** 638-644.

King EO, Ward MK, Raney DE (1954). Two simple media for the demonstration of pyocyanin and fluorescin. *J Lab Clin Med* **44:** 301-307.

Krupa S, Bowersox V, Claybrooke R, Barnes CW, Szabo L, Harlin K *et al* (2006). Introduction of Asian soybean rust urediniospores into the Midwestern United States - A case study. *Plant Dis* **90:** 1254-1259.

Kunkeaw S, Tan S, Coaker G (2010). Molecular and Evolutionary Analyses of *Pseudomonas syringae* pv. *tomato* Race 1. *Mol Plant Microbe In* **23:** 415-424.

Lee BK, Hong SH, Lee DS (2000). Chemical composition of precipitation and wet deposition of major ions on the Korean peninsula. *Atmos Environ* **34:** 563-575.

Leyronas C, Nicot PC (2013). Monitoring viable airborne inoculum of *Botrytis cinerea* in the South-East of France over 3 years: relation with climatic parameters and the origin of air masses. *Aerobiologia* **29:** 291–299.

Lighthart B (1997). The ecology of bacteria in the alfresco atmosphere. *FEMS Microbiol Ecol* **23:** 263-274.

Lighthart B (1999). An hypothesis describing the general temporal and spatial distribution of alfresco bacteria in the earth's atmospheric surface layer. *Atmos Environ* **33:** 611-615.

Lindemann J, Constantinidou HA, Barchet WR, Upper CD (1982). Plants as sources of airborne bacteria, including ice nucleation active bacteria. *Appl Env Microbiol* **44:** 1059-1063.

Lindow SE (1983). The role of bacterial ice nucleation in frost injury to plants. *Annu Rev Phytopathol* **21:** 363-384.

Loye-Pilot MD, Morelli J (1988). Fluctuations of ionic composition of precipitations collected in Corsica related to changes in the origins of incoming aerosols. *J Aerosol Sci* **19:** 577-585.

Maki T, Susuki S, Kobayashi F, Kakikawa M, Yamada M, Higashi T *et al* (2008). Phylogenetic diversity and vertical distribution of a halobacterial community in the atmosphere of an Asian dust (KOSA) source region, Dunhuang City. *Air Qual Atmos Health* **1:** 81-89.

Manteau S, Abouna S, Lambert B, Legendre L (2003). Differential regulation by ambient pH of putative virulence factor secretion by the phytopathogenic fungus *Botrytis cinerea*. *FEMS Microbiol Ecol* **43:** 359-366.

Mazzaglia A, Studholme DJ, Taratufolo MC, Cai R, Almeida NF, Goodman T *et al* (2012). Pseudomonas syringae pv. actinidiae (PSA) Isolates from Recent Bacterial Canker of Kiwifruit Outbreaks Belong to the Same Genetic Lineage. *PLoS One* **7**.

Mircea M, Stefan S, Fuzzi S (2000). Precipitation scavenging coefficient: influence of measured aerosol and raindrop size distributions. *Atmos Environ* **34:** 5169-5174.

Mohan SK, Schaad NW (1987). An improved agar plating assay for detecting *Pseudomonas syringae* pv. *syringae* and *P. syringae* pv. *phaseolicola* in contaminated bean seed. *Phytopathology* **77:** 1390-1395.

Möhler O, Georgakopoulos DG, Morris CE, Benz S, Ebert V, Hunsmann S *et al* (2008). Heterogeneous ice nucleation activity of bacteria: new laboratory experiments at simulated cloud conditions. *Biogeosciences* **5:** 1425-1435.

Monier JM, Lindow SE (2003). *Pseudomonas syringae* responds to the environment on leaves by cell size reduction. *Phytopathology* **93:** 1209-1216.

Monteil CL, Guilbaud C, Glaux C, Lafolie F, Soubeyrand S, Morris CE (2012). Emigration of the plant pathogen *Pseudomonas syringae* from leaf litter contributes to its population dynamics in alpine snowpack. *Environ Microbiol* **14:** 2099-2112.

Morris CE, Sands DC, Vinatzer BA, Glaux C, Guilbaud C, Buffiere A *et al* (2008). The life history of the plant pathogen *Pseudomonas syringae* is linked to the water cycle. *ISME J* **2:** 321-334.

Morris CE, Sands DC, Vanneste JL, Montarry J, Oakley B, Guilbaud C *et al* (2010). Inferring the evolutionary history of the plant pathogen *Pseudomonas syringae* from its biogeography in headwaters of rivers in North America, Europe, and New Zealand. *mBio* **1:** 1 - 10.

Morris CE, Conen F, Huffman JA, Phillips V, Pöschl U, Sands DC (2014a). Bioprecipitation: Feedbacks linking Earth history, ecosystem dynamics and land use through biological ice nucleators in the atmosphere. *Global Change Biol* **20:** 341-351.

Morris CE, Leyronas C, Nicot PC (2014b). Movement of Bioaerosols in the Atmosphere and the Consequences for Climate and Microbial Evolution In: Colbeck I, Lazaridis M (eds). *Aerosol Science: Technology and Applications*. John Wiley & Sons, Ltd. pp 393-416.

Nagarajan S, Singh DV (1990). Long-distance dispersion of rust pathogens. *Annu Rev Phytopathol* **28:** 139-153.

Oki T, Kanae S (2006). Global hydrological cycles and world water resources. *Science* **313:** 1068-1072.

Ozsoy T, Saydam AC (2000). Acidic and alkaline precipitation in the Cilician Basin, north-eastern Mediterranean Sea. *Sci Total Environ* **253:** 93-109.

Pan Z, Yang XB, Pivonia S, Xue L, Pasken R, Roads J (2006). Long-term prediction of soybean rust entry into the continental United States. *Plant Dis* **90:** 840-846.

Pezet R, Pont V (1990). Ultrastructural observations of pterostilbene fungotoxicity in dormant conidia of *Botrytis cinerea* Pers. *J Phytopathol* **129:** 19-30.

Pfender W, Graw R, Bradley W, Carney M, Maxwell L (2006). Use of a complex air pollution model to estimate dispersal and deposition of grass stem rust urediniospores at landscape scale. *Agr Forest Meteorol* **139:** 138-153.

Pritchard JK, Stephens M, Donnelly P (2000). Inference of population structure using multilocus genotype data. *Genetics* **155:** 945-959.

Prospero JM, Blades E, Mathison G, Naidu R (2005). Interhemispheric transport of viable fungi and bacteria from Africa to the Caribbean with soil dust. *Aerobiologia* **21:** 1-19.

Pruppacher HR, Klett JD (1997). *Microphysics of clouds and precipitation.* Kluwer Academic Publishers: Dordrecht.

Purdy LH, Krupa SV, Dean JL (1985). Introduction of sugarcane rust into the Americas and its spread to Florida *Plant Dis* **69:** 689-693.

Quantum GIS Development Team (2011). Quantum GIS Geographic Information System. In: Project. OSGF (ed).

Riffaud CMH, Morris CE (2002). Detection of *Pseudomonas syringae* pv. *aptata* in irrigation water retention basins by immunofluorescence colony-staining. *Eur J Plant Pathol* **108:** 539-545.

Rodhe H, Grandell J (1972). On the removal time of aerosol particles from the atmosphere by precipitation scavenging. *Tellus* **24:** 442–454.

Rogers RR, Yau MK (1989). *A Short Course in Cloud Physics*. Pergamon Press: Series in Nat. Phil. Oxford

Sands DC, Schroth MN, Hildebrand DC (1970). Taxonomy of phytopathogenic pseudomonads. *J Bacteriol* **101:** 9-23.

Sands DC, Langhans VE, Scharen AL, de Smet G (1982). The association between bacteria and rain and possible resultant meteorogical implications. *J Hungarian Meteorol Ser* **86:** 148-152.

Sarkar SF, Guttman DS (2004). Evolution of the core genome of *Pseudomonas syringae*, a highly clonal, endemic plant pathogen. *Appl Env Microbiol* **70:** 1999-2012.

Smith DJ, Timonen HJ, Jaffe DA, Griffin DW, Birmele MN, Perry KD *et al* (2013). Intercontinental Dispersal of Bacteria and Archaea by Transpacific Winds. *Appl Env Microbiol* **79:** 1134-1139.

Tao Z, Malvick D, Claybrooke R, Floyd C, Bernacchi CJ, Spoden G *et al* (2009). Predicting the risk of soybean rust in Minnesota based on an integrated atmospheric model. *Int J Biometeorol* **53:** 509-521.

The R Development Core Team (2011). R: A language and environment for statistical computing. Vienna, Austria: R Foundation for Statistical Computing. ISBN: 3-900051-07-0.

Tong YY, Lighthart B (2000). The annual bacterial particle concentration and size distribution in the ambient atmosphere in a rural area of the Willamette valley, Oregon. *Aerosol Sci Tech* **32:** 393-403.

Wang H, Yang XB, Ma Z (2010). Long-distance spore transport of wheat stripe rust pathogen from Sichuan, Yunnan, and Guizhou in Southwestern China. *Plant Dis* **94:** 873-880.

Webber JF, Parkinson NM, Rose J, Stanford H, Cook RTA, al. e (2008). Isolation and identification of *Pseudomonas syringae* pv. *aesculi* causing bleeding canker of horse chestnut in the UK. . *Plant Pathol New Dis Rep* **15**.

Williamson B, Tudzynsk B, Tudzynski P, van Kan JAL (2007). *Botrytis cinerea*: the cause of grey mould disease. *Mol Plant Pathol* **8:** 561-580.

Wolber PK, Deininger CA, Southworth MW, Vandekerckhove J, Vanmontagu M, Warren GJ (1986). Identification and purification of a bacterial ice nucleation protein. *Proc Natl Acad Sci USA* **83:** 7256-7260.

Zhu M, Radcliffe EB, Ragsdale DW, MacRae IV, Seeley MW (2006). Low-level jet streams associated with spring aphid migration and current season spread of potato viruses in the US northern Great Plains. *Agr Forest Meteorol* **138:** 192-202.

FIGURE LEGEND

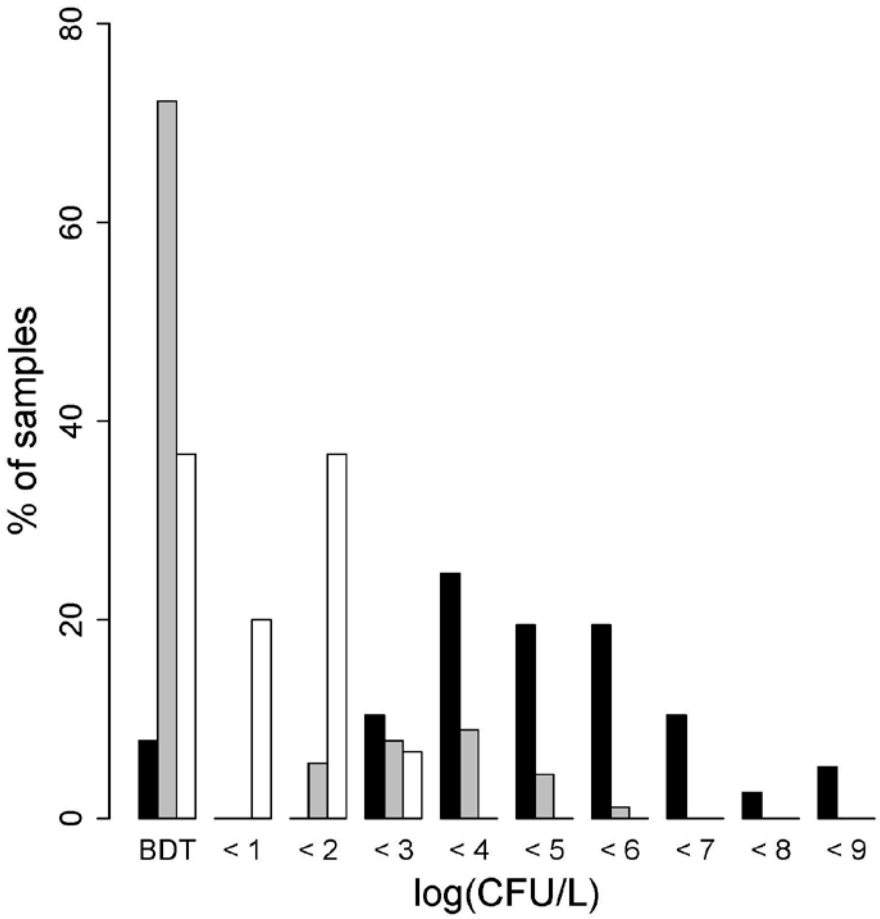

Figure 1 Population densities of total culturable bacteria, *P. syringae* and *B. cinerea* in rainfall and snowfall. Black, grey and white bars represent total culturable bacteria, *P. syringae* and *B. cinerea* respectively. BDT means "under Bacterial Detection Threshold".

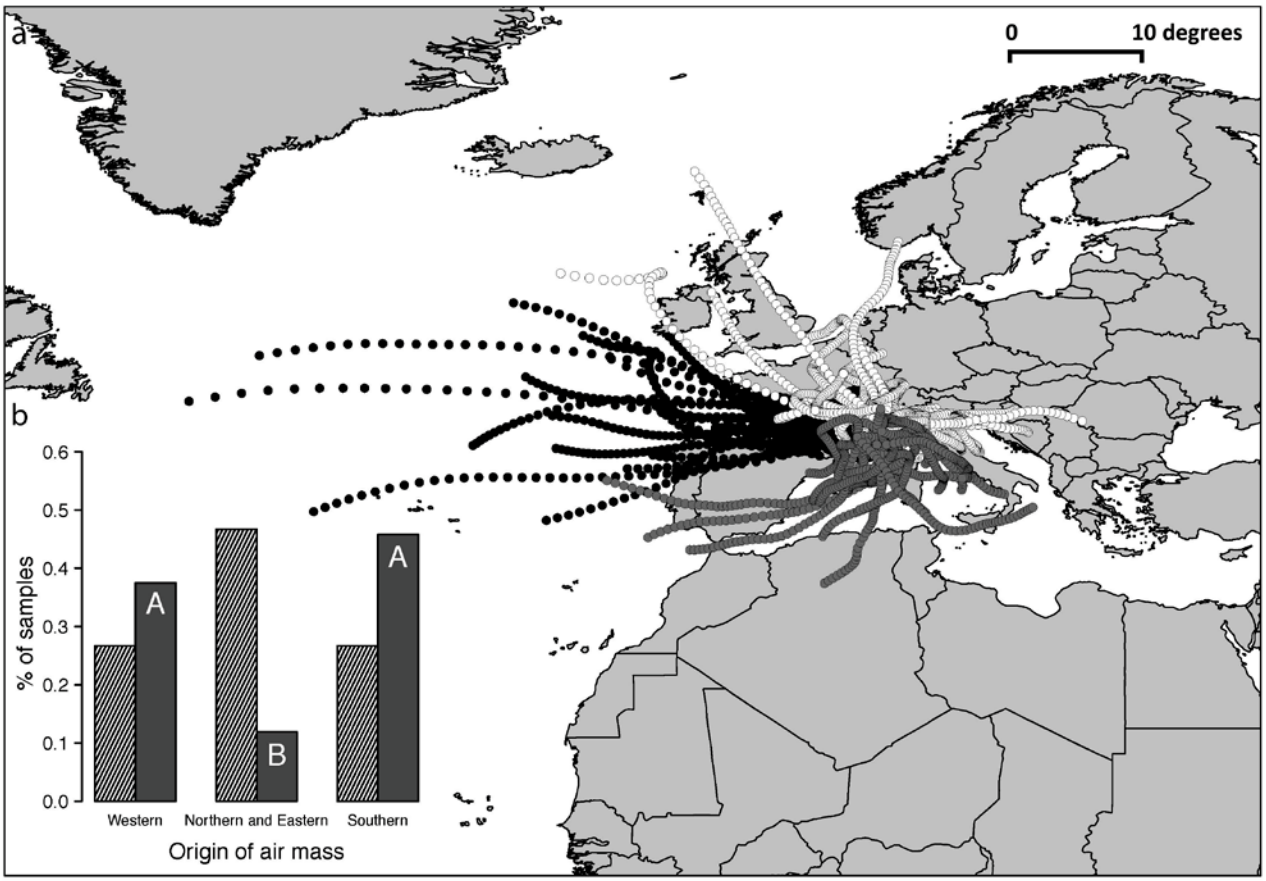

Figure 2 Occurrence of *P. syringae* in precipitation according to the origin of air masses. (**a**) Backward trajectories of air masses associated with the 90 precipitation samples are plotted for the 48 h preceding the sampling for the 500 m above the ground level (a.g.l). Each circle corresponds to a spatial coordinate for each hour. Each air mass trajectory was classified according to the three geographical sectors defined by Celle-Jeanton *et al.* (2009) for precipitations in Southeastern France: West (●), North and East (○) and Mediterranean (●). (**b**) Precipitation frequencies coming from these three sectors are represented by hatched bars. Grey bars represent frequencies of samples carrying *P. syringae* for each origin. Values associated with the same letter are not significantly different (Multiple Fisher-exact test, $P < 0.05$).

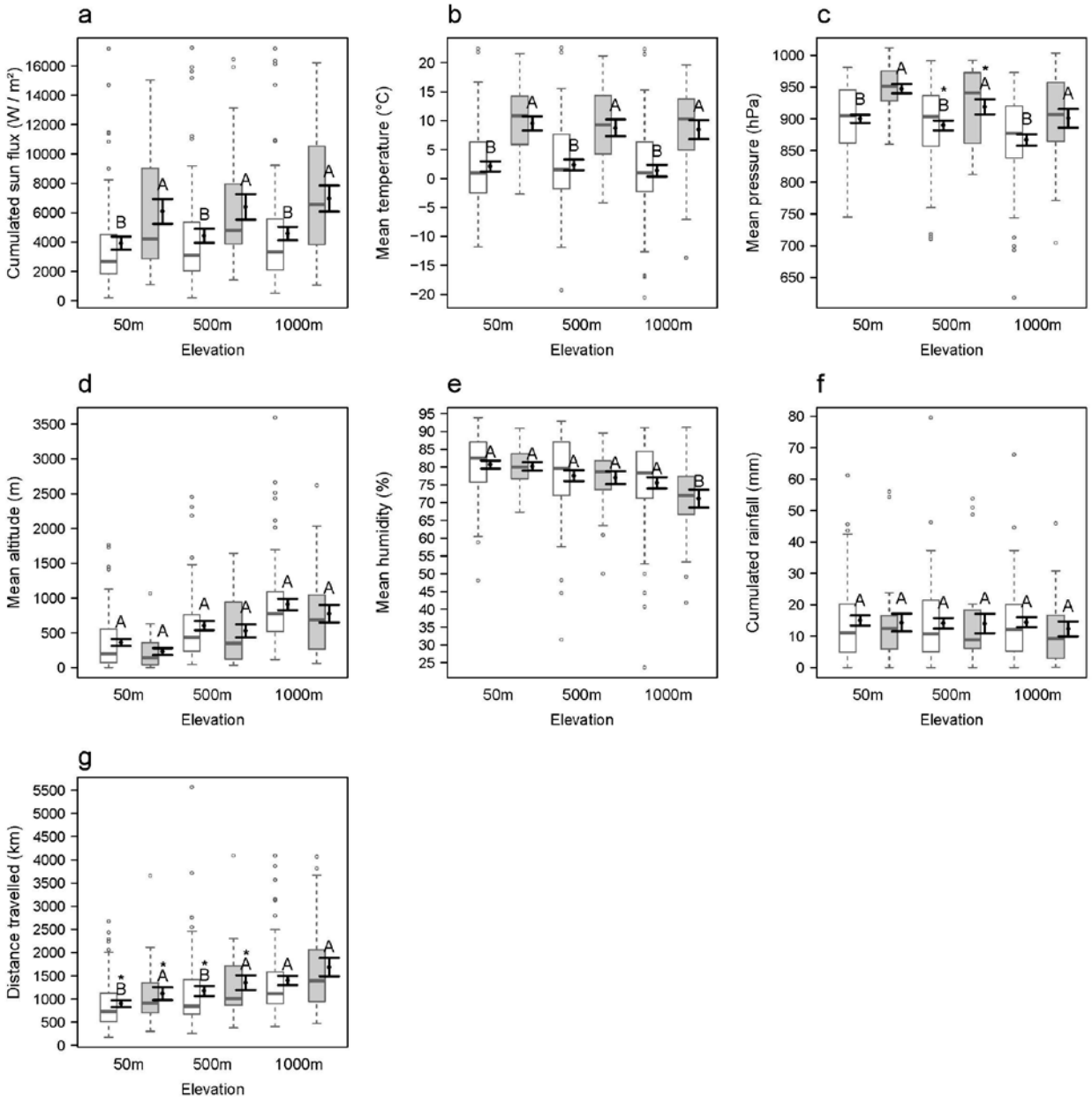

Figure 3 Physical properties of air masses carrying *P. syringae* during 48 h preceding the precipitation event. Aggregate mean of properties of air masses [cumulated sun flux (**a**), mean temperature (**b**), mean pressure (**c**), mean altitude (**d**), mean humidity (**e**), cumulated rainfall (**f**) and distance travelled (**g**)] are compared between precipitations that carried *P. syringae* (grey boxes) and those that did not carry *P. syringae* (white boxes). Comparisons were performed for each elevation (50m, 500m and 1000m). The mean with its standard error are presented next to each box plot. Values associated with the same letter are not significantly different (n=90, MWU test, $P < 0.05$).

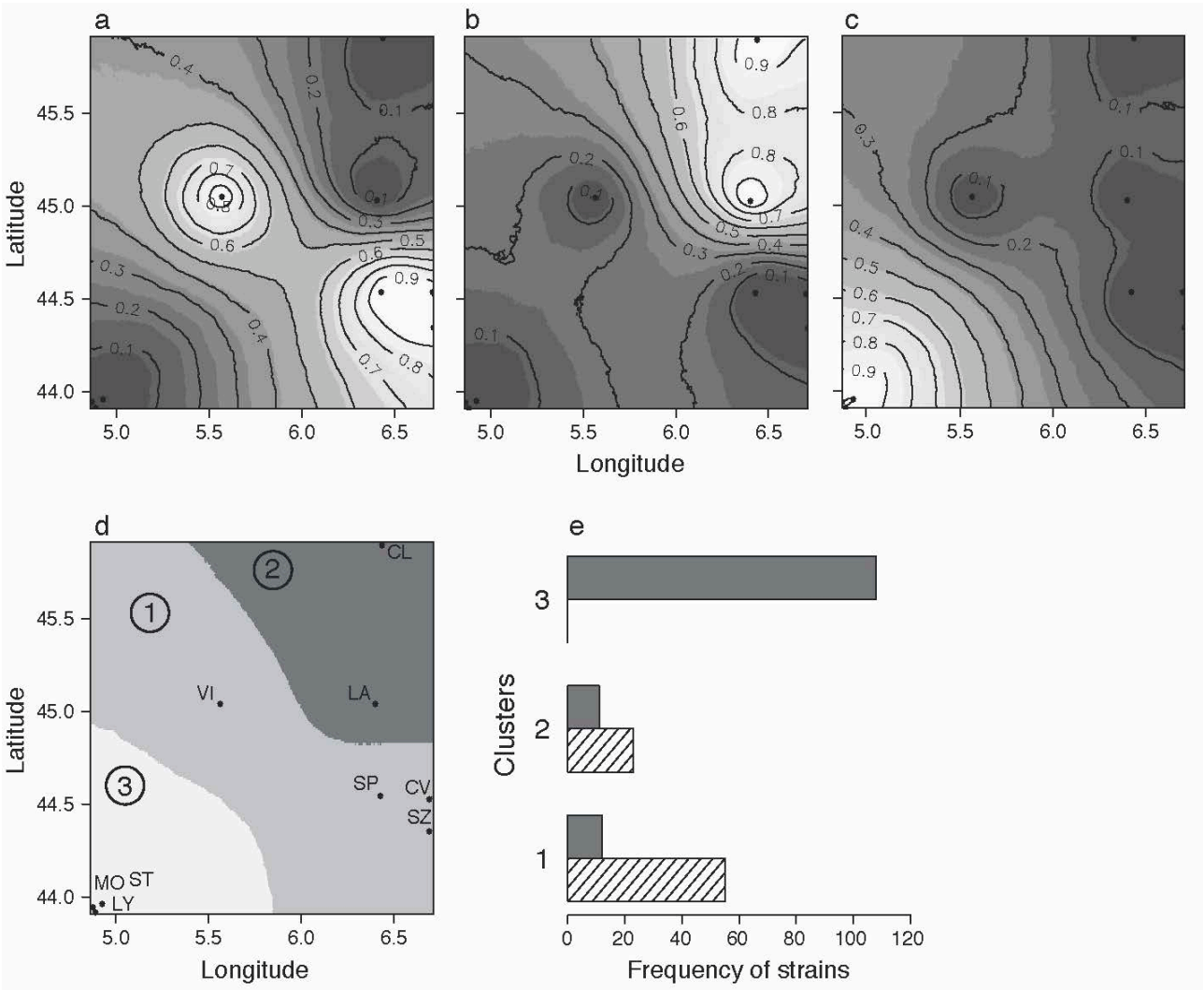

Figure 4 Population structure of *P. syringae* over the study area. The computation was performed with *cts* sequence polymorphism and spatial distribution of individuals, considering the uncorrelated allele frequency model. (**a-c**) Maps of posterior probability for each pixel of the study area to belong to the panmictic clusters identified: cluster 1, cluster 2 and cluster 3 respectively. A grey-to-white graded scale represents probabilities from 0 to 1 and sampling sites are represented by black dots. (**d**) Map of cluster membership to the study area of the three clusters. Clusters are represented by a different color and sampling site names are associated with black dots (CV, Col de Vars; CL, La Clusaz; LA, Col du Lautaret; LY, Montfavet St Paul; MO, Montfavet St Maurice; SP, Savines le Lac; ST, St Saturnin les Avignon; SZ, Super Sauze; VI, Villars de Lans). (**e**) The estimated membership value of each strain to each *k* cluster according to the type of precipitation: snow (hatched bars) or rain (grey bars). All the strains were assigned to clusters with a probability > 0.99.

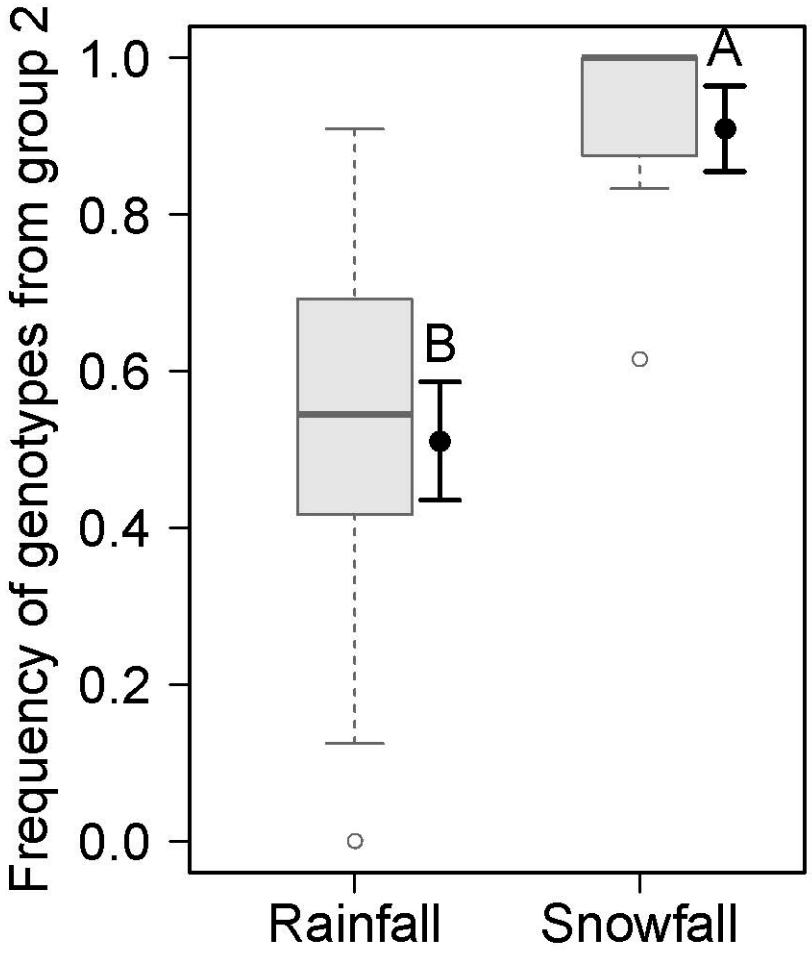

Figure 5 Frequency of strains belonging to phylogroup 2 in snow and rain. The mean and its standard error are indicated next to each box plot. Values associated with the same letter are not significantly different (n=19, MWU test, $P < 0.05$).

Table 1 Sampling sites and number of samples collected

County	Site	Latitude[a]	Longitude	Altitude (m)	Number of samples	
					Snow	Rain
Alpes de Haute Provence	Col de Vars	44.537	6.702	2100	4	0
	Savines le Lac	44.539	6.426	830	0	1
	Super Sauze	44.349	6.710	2000	38	0
Bouches-du-Rhône	Châteaurenard	43.881	4.859	55	0	2
Haute Savoie	La Clusaz	45.906	6.436	1104	1	0
	Les Carroz d'Araches	46.026	6.638	1111	2	0
Hautes Alpes	Ceillac	44.636	6.790	2200	7	0
	Col du Lautaret	45.036	6.402	2100	4	1
Isère	Villars de Lans	45.052	5.564	1200	2	0
Pyrénnées Orientales	Font Romeu, Aveillans	43.521	2.063	1780	1	0
	Font Romeu, Roc de la Calme	42.505	2.042	1104	1	0
Savoie	Saint-François Longchamp	45.410	6.348	1700	1	0
Vaucluse	Montfavet, St Maurice	43.946	4.864	25	1	6
	Montfavet, St Paul	43.916	4.882	30	0	2
	St. Saturnin-les-Avignon	43.959	4.923	83	3	13

[a] GPS coordonates were converted in decimal degrees.

Table 2 Physical properties of air masses carrying *P. syringae* during the 24h, 48h and 120h preceding the precipitation event. HYSPLIT estimated the climatic data associated with the air masses at each hour of the backward trajectories for the tree endpoint elevations (50, 500 or 100 m above the ground level). The sum, the minimum, maximum, and mean of the hourly physical properties of air masses were calculated for durations of 24h, 48h and 120h. Aggregate means of each variable were compared between air masses having produced precipitations in which *P. syringae* was detected versus the ones in which *P. syringae* was not detected. Means are associated with their standard errors. Values were significantly different when they were colored in light grey (MWU test, $P < 0.1$) or in dark grey (MWU test, $P < 0.05$). Arrows go from the upper value to the lower.

	24h backward trajectories								
	50m			500m			1000m		
Physical parameter	Present		*Absent*	Present		*Absent*	Present		*Absent*
Sum of sun flux (W / m²)									
	2766 ± 434	→	*1842 ± 228*	2956 ± 438	→	*2015 ± 247*	3372 ± 472	→	*2117 ± 240*
Temperature (°C)									
Min	4.2 ± 1.4	→	*-3.3 ± 0.9*	2.7 ± 1.4	→	*-5.1 ± 0.9*	1.0 ± 1.5	→	*-7.3 ± 0.9*
Max	12.5 ± 1.2	→	*5.8 ± 0.9*	12.3 ± 1.2	→	*6.4 ± 0.9*	12.4 ± 1.3	→	*5.8 ± 0.9*
Mean	8.6 ± 1.2	→	*1.4 ± 0.9*	8.5 ± 1.4	→	*1.4 ± 0.9*	8.3 ± 1.5	→	*0.5 ± 0.9*
Pressure (hPa)									
Min	870 ± 12	→	*818 ± 7*	828 ± 12	→	*770 ± 7*	789 ± 12	→	*732 ± 8*
Max	982 ± 6	→	*950 ± 6*	966 ± 8	→	*946 ± 7*	957 ± 10	→	*926 ± 8*
Mean	933 ± 8	→	*889 ± 6*	916 ± 11	→	*874 ± 8*	900 ± 13	→	*851 ± 8*
Altitude (m agl)									
Min	22 ± 5	→	*19 ± 3*	180 ± 38	←	*227 ± 26*	376 ± 67	←	*484 ± 44*
Max	407 ± 68	←	*521 ± 65*	830 ± 87	←	*994 ± 66*	1252 ± 95	←	*1403 ± 75*
Mean	204 ± 46	←	*270 ± 42*	444 ± 76	←	*575 ± 54*	706 ± 101	←	*880 ± 60*
Relative humidity (%)									
Min	72.1 ± 2.0	→	*70.1 ± 1.7*	66.2 ± 2.4	→	*66.7 ± 2.1*	61.6 ± 3.3	←	*64.2 ± 2.2*
Max	93.6 ± 1.0	←	*93.8 ± 0.8*	93.7 ± 0.9	→	*93.0 ± 1.3*	93.8 ± 1.5	→	*92.7 ± 1.3*
Mean	83.3 ± 1.4	=	*83.3 ± 1.2*	79.8 ± 1.5	←	*80.8 ± 1.6*	76.7 ± 2.2	←	*78.7 ± 1.8*
Sum of Rainfall (mm)									
	9.9 ± 1.7	←	*10.4 ± 1.1*	10.1 ± 2.2	→	*9.8 ± 1.2*	9.8 ± 2.1	←	*10.5 ± 1.4*
Distance traveled (km)									
	476 ± 44	→	*393 ± 31*	622 ± 53	→	*576 ± 53*	810 ± 75	→	*677 ± 52*

	48h backward trajectories								
	50m			500m			1000m		
Physical parameter	Present		*Absent*	Present		*Absent*	Present		*Absent*
Sum of sun flux (W / m²)									
	6087 ± 847	→	*3925 ± 447*	6394 ± 866	→	*4427 ± 476*	6961 ± 884	→	*4580 ± 461*
Temperature (°C)									
Min	3.4 ± 1.5	→	*-4.2 ± 0.9*	1.3 ± 1.8	→	*-5.6 ± 0.9*	-0.3 ± 1.8	→	*-8.4 ± 1.1*
Max	14.1 ± 1.1	→	*7.0 ± 0.9*	13.8 ± 1.2	→	*7.9 ± 0.9*	13.3 ± 1.4	→	*7.7 ± 0.9*
Mean	9.5 ± 1.2	→	*2.1 ± 0.9*	8.7 ± 1.4	→	*2.3 ± 0.9*	8.4 ± 1.6	→	*1.3 ± 1.0*
Pressure (hPa)									
Min	863 ± 12	→	*803 ± 7*	*816 ± 14*	→	*766 ± 7*	*774 ± 14*	→	*724 ± 8*
Max	992 ± 6	→	*965 ± 5*	976 ± 7	→	*962 ± 6*	963 ± 10	→	*946 ± 7*
Mean	947 ± 8	→	*900 ± 6*	919 ± 12	→	*889 ± 8*	*901 ± 15*	→	*867 ± 9*

Altitude (m agl)									
Min	19 ± 4	→	*18 ± 3*	162 ± 37	←	*173 ± 24*	334 ± 66	←	*375 ± 45*
Max	535 ± 77	←	*794 ± 76*	1099 ± 145	←	*1154 ± 84*	1516 ± 156	←	*1620 ± 105*
Mean	232 ± 49	←	*362 ± 51*	528 ± 95	←	*605 ± 66*	776 ± 126	←	*907 ± 82*
Relative humidity (%)									
Min	64.5 ± 1.8	→	*61.2 ± 2.0*	58.3 ± 3.4	→	*58.1 ± 2.2*	54.5 ± 3.5	←	*56.0 ± 2.1*
Max	94.8 ± 0.8	←	*95.3 ± 0.7*	94.5 ± 0.9	←	*94.6 ± 1.2*	94.3 ± 1.5	←	*94.7 ± 1.0*
Mean	80.2 ± 1.2	←	*80.7 ± 1.1*	77.0 ± 1.8	←	*77.6 ± 1.5*	71.1 ± 2.5	←	*75.6 ± 1.6*
Sum of Rainfall (mm)									
	14.3 ± 2.8	←	*15.0 ± 1.6*	14.0 ± 3.1	←	*14.1 ± 1.7*	12.3 ± 2.4	←	*14.5 ± 1.6*
Distance traveled (km)									
	1116 ± 139	→	*898 ± 72*	1354 ± 160	→	*1173 ± 108*	1689 ± 196	→	*1402 ± 102*

	120h backward trajectories					
	50m		500m		1000m	
Physical parameter	Present	*Absent*	Present	*Absent*	Present	*Absent*
Sum of sun flux (W / m²)						
	15917 ± 2057 →	*10702 ± 1054*	16718 ± 2214 →	*10863 ± 1093*	17655 ± 2146 →	*11135 ± 1147*
Temperature (°C)						
Min	-4.4 ± 2.8 →	*-11.2 ± 1.5*	-8.7 ± 3.3 →	*-14.5 ± 1.6*	-12.8 ± 3.5 →	*-15.8 ± 1.9*
Max	15.1 ± 1.0 →	*9.1 ± 0.9*	15.0 ± 1.2 →	*9.5 ± 0.9*	14.3 ± 1.4 →	*9.3 ± 1.0*
Mean	6.8 ± 1.8 →	*0.8 ± 1.0*	5.6 ± 2.3 →	*0.0 ± 1.1*	3.7 ± 2.4 →	*-1.2 ± 1.3*
Pressure (hPa)						
Min	*798 ± 21* →	*736 ± 13*	723 ± 24 →	*682 ± 14*	665 ± 29 ←	*667 ± 15*
Max	*1002 ± 6* →	*981 ± 5*	990 ± 8 →	*976 ± 6*	970 ± 10 →	*968 ± 7*
Mean	*930 ± 13* →	*889 ± 9*	*896 ± 19* →	*867 ± 11*	856 ± 24 →	*856 ± 12*
Altitude (m agl)						
Min	14 ± 4 =	*14 ± 3*	136 ± 35 ←	*140 ± 23*	293 ± 64 →	*275 ± 40*
Max	1354 ± 245 ←	*1828 ± 185*	2141 ± 326 ←	*2378 ± 191*	2812 ± 398 →	*2437 ± 192*
Mean	508 ± 118 ←	*721 ± 87*	885 ± 191 ←	*997 ± 100*	1286 ± 232 →	*1142 ± 115*
Relative humidity (%)						
Min	51 ± 3 →	*46.4 ± 2.3*	40.8 ± 3.5 →	*40.6 ± 2.5*	36.2 ± 4.0 ←	*41.6 ± 2.6*
Max	96.5 ± 0.7 ←	*96.8 ± 0.5*	95.7 ± 0.8 ←	*96.8 ± 0.6*	96.6 ± 0.9 ←	*97.1 ± 0.7*
Mean	76.6 ± 1.5 →	*75.0 ± 1.4*	70.7 ± 1.8 ←	*71.6 ± 1.4*	65.7 ± 2.5 ←	*72.8 ± 1.4*
Sum of Rainfall (mm)						
	20.5 ± 3.81 ←	*22.4 ± 2.1*	20.1 ± 3.9 ←	*23.9 ± 2.5*	17.8 ± 2.6 ←	*21.7 ± 1.9*
Distance traveled (km)						
	3386 ± 378 →	*2993 ± 193*	4061 ± 459 →	*3659 ± 249*	4534 ± 537 →	*4058 ± 246*

Table 3 Frequency of precipitations carrying *P. syringae* and *B. cinerea*. The subsample corresponded to the precipitation samples for which both microorganisms were quantified. Values associated with the same letter were not significantly different (Multiple Fisher-exact test, $P < 0.05$). Frequencies were compared either by organism (capital letters) or by the type of precipitation (lowercase letters).

		Frequency of samples carrying the target microorganism (%)		
Samples set used	Plant pathogen	All precipitation	Rain	Snow
Whole sample (n=90)				
	P. syringae	$27.8^{B\ bc}$	$68.0^{A\ a}$	$12.3^{C\ bc}$
Subsample (n=29)				
	P. syringae	$34.5^{AB\ b*}$	$53.8^{A\ a}$	$18.8^{B*\ b}$
	B. cinerea	$62.1^{A\ a}$	$76.9^{A\ a}$	$50.0^{A\ a}$

* Differences significants on a treeshold of P < 0.06 according the Fisher Exact test

Table 4 Population characteristics of *P. syringae* and *B. cinerea* in precipitation. Means of population sizes, frequencies of phenotypes or freezing temperature were compared between rainfall and snowfall with either a Student t-test (T) or the non parametric MWU test (M) if data did not follow a normal distribution.

Parameter	Mean ± SE		test	P value
	Rain	Snow		
Total bacteria				
Population size (log (CFU L^{-1}))	5.30 ± 0.31	4.52 ± 0.22	M	0.03
Pseudomonas syringae				
Population size (log (CFU L^{-1}))	2.77 ± 0.19	3.66 ± 0.40	T	0.07
Frequency of INA[1] strains (%)	59.5 ± 7.0	100 ± 0.0	M	0.002
Temperature of ice nucleation activity (°C)	−4.03 ± 0.05	−4.07 ± 0.05	M	0.58
Frequency of strains inducing HR (%)	78.0 ± 7.5	100 ± 0.0	M	0.0003
Frequency of strains consuming D(–)tartrate (%)	29.3 ± 5.8	2.2 ± 2.0	M	0.002
Botrytis cinerea				
Population size (log (CFU L^{-1}))	1.26 ± 0.17	1.30 ± 0.30	T	0.91
Frequency of INA strains (%)	no ice nucleation activity detected			
Aggressiveness index (% BC1)	62.25 ± 3.58	63.72 ± 8.02	M	0.74

[1]Ice nucleation active

Table 5 Frequency of ice nucleation active strains in precipitation in relation to the frequency of strains inducing hypersensitivity (HR) on tobacco and air mass properties. All the correlations with physical properties listed in Material and Methods have been tested for the three durations and the three elevations. Only variables for which at least one of the Pearson or Spearman coefficients was significantly different from zero are presented ($P < 0.1$).

Variables*	**Linear model (method of least squares)**		**Pearson's rank correlation test**		**Spearman's rank correlation test**	
	Model	*F*-statistics	*cor*	P value	*rho*	P value
Frequency of HR strains (%)	$y = 0.61\,x + 0.40$	18.55	0.72	0.0005	0.79	10^{-5}
For air masses at 24 h						
Min air pressure						
50 m	$y = -72\,x + 916$	2.628	–0.37	0.12	–0.48	0.04
500 m	$y = -92\,x + 886$	0.038	–0.41	0.06	–0.29	0.23
1000 m	$y = -90\,x + 846$	3.429	–0.41	0.08	–0.46	0.04
Sum sun flux						
1000 m	$y = -3102\,x + 5423$	3.05	–0.39	0.1	–0.53	0.02
For air masses at 48 h						
Min air pressure						
50 m	$y = -71\,x + 912$	3.094	–0.39	0.09	–0.48	0.03
500 m	$y = -103\,x + 879$	3.72	–0.42	0.07	–0.36	0.12
1000 m	$y = -82\,x + 826$	1.805	–0.31	0.20	–0.40	0.09
Sum sun flux						
1000 m	$y = -5{,}542\,x + 10{,}416$	2.821	–0.38	0.11	–0.57	0.01
Min temperature						
500 m	$y = -11.7\,x + 7.9$	2.905	–0.38	0.11	–0.48	0.04
Distance travelled						
500 m	$y = 1440\,x + 431$	4.829	0.47	0.04	0.60	0.006
1000 m	$y = 1817\,x + 422$	7.001	0.54	0.02	0.64	0.003
For air masses at 120 h						
Sum sun flux						
1000 m	$y = -14{,}917\,x + 27{,}071$	3.281	–0.40	0.09	–0.50	0.03
Distance travelled						
500 m	$y = 3264\,x + 1977$	2.772	–0.33	0.17	0.45	0.05

* based on the analyse of n = 19 samples